# Particle size and magnetic field dependent resistivity and thermoelectric power of La0.5Pb0.5MnO3 above and below metal–insulator transition

Aritra Banerjee, Sudipta Pal, S. Bhattacharya, B. K. Chaudhuri, and H. D. Yang

Citation: J. Appl. Phys. **91**, 5125 (2002); doi: 10.1063/1.1459618
View online: http://dx.doi.org/10.1063/1.1459618
View Table of Contents: http://jap.aip.org/resource/1/JAPIAU/v91/i8
Published by the American Institute of Physics.

# Particle size and magnetic field dependent resistivity and thermoelectric power of $La_{0.5}Pb_{0.5}MnO_3$ above and below metal–insulator transition

Aritra Banerjee, Sudipta Pal, S. Bhattacharya, and B. K. Chaudhuri[a)]
*Solid State Physics Department, Indian Association for the Cultivation of Science, Kolkata 700032, India*

H. D. Yang
*Department of Physics, National Sun Yat-Sen University, Kaohsiung, Taiwan 804, Republic of China*

(Received 11 September 2001; accepted for publication 17 January 2002)

The effect of particle size on the transport properties (resistivity and thermopower) of $La_{0.5}Pb_{0.5}MnO_3$ has been investigated both in the presence and in the absence of magnetic field $B=0.0-1.5$ T (maximum). Grain size, dc conductivity; and the metal–insulator transition temperature $T_p$ of the sample increase with increasing annealing time. Grain size has, however, comparatively little effect on the Seebeck coefficient $S$. Magnetoresistance is higher for the samples with smaller grain sizes. dc magnetic susceptibility also increases with increasing grain size. High temperature ($T>\theta_D/2$) resistivity data well fit the small polaron hopping model. Polaron hopping energy $W_H$ decreases but polaron radius $r_p$ increases with the increase of grain size. In the metallic regime (for $T<T_p$), resistivity data fit well with $\rho=\rho_0+\rho_{2.5}\,T^{2.5}$ and the transport mechanism is attributed mainly to the magnon-carrier scattering ($\sim T^{2.5}$). In all the samples with different grain sizes, $S$ changes sign below $T_p$. In contrast to magnetoresistance, application of magnetic field increases $S$ at low temperature ($T<T_p$) for these samples. Thermopower data in the metallic phase (both for $B=0.0$ and 1.5 T) can be analyzed by considering a spin-wave fluctuation term ($\sim T^4$) in addition to the magnon-scattering term similar to the case of resistivity data. Although the variable range hopping mechanism is supported from the resistivity data (for $T_p>T>\theta_D/2$), it is hard to justify this model from the temperature dependent thermopower data. © *2002 American Institute of Physics.* [DOI: 10.1063/1.1459618]

## I. INTRODUCTION

The phenomenon of giant magnetoresistance (GMR) in $La_{1-x}A_xMnO_3$ ($A$=Sr,Ba,Ca,Pb) has spurred renewed interest because of their interesting physical properties[1–3] and also for their uses in the field of magnetic memory sensor, recorder heads, etc. Previously several attempts have been made to explain the magnetotransport property and metal–insulator transition (MIT) considering the double exchange (DE) mechanism.[4] It is now established that the DE mechanism alone cannot explain the available experimental data. The contribution of electron–phonon interaction leading to the Jahn–Teller mechanism has also been invoked.[5] So far structural and magnetotransport properties of single crystals, thin films, and polycrystalline powders of these doped manganites have been studied in detail.[6–8] But the role of grain boundaries and the effect of grain size on the magnetotransport property including thermopower have not yet been clearly revealed.[9–11] For technological application of these manganites, it is of fundamental importance to investigate the effect of particle size on the magnetoresistance (MR), thermoelectric power (TEP), and other properties. In the low temperature metallic phase, like resistivity, TEP is also related to the changes in electronic structure and different scattering processes. Again in the high temperature insulating (semiconducting) phases, TEP and MR data provide important information on the energy dependence of the parameters governing the high temperature charge transport mechanism.

In the present work we have carefully investigated and analyzed the effect of particle size on the magnetotransport properties of a typical concentration of the well characterized La–Pb–Mn–O-type GMR system[3,12] viz, $La_{0.5}Pb_{0.5}MnO_3$ by measuring the temperature and magnetic field (maximum field $B=1.5$ T) dependent resistivity, thermoelectric power, and related parameters.

## II. EXPERIMENT

Polycrystalline $La_{0.5}Pb_{0.5}MnO_3$ samples with different grain size were prepared by the conventional solid state reaction method.[13,14] Several successive steps, as mentioned below, are taken to make samples of different grain sizes. Stoichiometric amounts of $La_2(CO_3)_3$, PbO, and $Mn(C_2H_3O_2)$ (each of purity >99.99%) were first well mixed and heated at 500 °C for 5 h. This precursor sample is divided into three parts for making three samples of different grain sizes (S1<S2<S3). After well grounding, the first part (S1) is heated at 900 °C for 48 h with intermediate grinding. The grounded powder was palletized and annealed again at 900 °C for 24 h. For preparing the next sample (S2), the second part of the precursor powder was sintered at 900 °C for 65 h with intermediate grounding (seven times). This annealed powder was next palletized and then annealed again at 900 °C for 24 h. To prepare the third sample (S3) of

a)Author to whom correspondence should be addressed; electronic mail: sspbkc@mahendra.iacs.res.in

 

the largest grain size (S3 > S2 > S1), the well ground preheated sample was sintered at 900 °C for 72 h with intermediate grounding after every 24 h. The well ground powder is then palletized and annealed at 940 °C for 25 h. All three sample pellets in their respective final stages were furnace cooled to room temperature. The phase purity of S1, S2, and S3 were checked by x-ray diffraction (XRD) with Cu $K_\alpha$ radiation ($\lambda = 1.541$ Å). The particle size was determined both from XRD and transmission electron microscope (TEM) techniques. For TEM study, finely powdered samples on carbon grids were used. Temperature dependent resistivity $[\rho(T)]$ was measured with four probe technique in the range of 80–400 K both in $B = 0.0$ and 1.5 T magnetic field. Temperature and field dependent thermoelectric power ($S$) was measured by the standard differential technique[14] in the temperature range of 80–300 K. All the experimental data were collected in the heating direction similar to our earlier work.[15] Room temperature (300 K) susceptibilities of the samples were measured by vibrating sample magnetometry.

## III. RESULTS AND DISCUSSION

The single-phase (perovskite-type) behavior of all the samples is confirmed from the XRD patterns shown in Fig. 1. From the XRD peak width we have calculated the grain size of each of the samples using the relation[16] $S = K\lambda/\beta\cos(\theta)$, where $K$ is a constant depending on the grain shape (=0.89, for circular grain), $\lambda$ = wavelength of Cu $K_\alpha$ radiation (=1.541 Å), and $\beta$ = full width at half maxima of the XRD peaks. From the estimated grain size, as shown in Table I, one find that grain size increases with increasing sample number, i.e., with increasing annealing time, temperature, and also grinding time. As the above method for determining grain size using XRD data is an approximate one and often corresponds to crystalline domain size inside each grain, we have also analyzed the samples using the TEM technique. The TEM micrographs shown in Fig. 2 clearly indicate the grain size differences (successive increase of grain size from S1 to S3) in these samples. The estimated average particle/grain sizes obtained from TEM micrographs shown in Table I also indicate that particle or grain size increases with annealing time. The effect of grain size on the transport property is discussed below.

### A. Grain size and field dependent resistivity

Figure 3 represents temperature and field dependent resistivity $[\rho(T)]$ of the samples of different grain sizes (S1, S2, S3) showing distinct maxima around the MIT temperature $T_p$. Unlike resistivity, room temperature paramagnetic susceptibility $\chi$ increases with the increase of grain size (Table I) which is in accordance with that of an earlier observation.[10] Figure 3 shows the systematic decrease of $\rho$ with increasing grain size over the whole range of temperature of our investigation. On the other hand $T_p$ increases with increasing grain size of the samples. This is not unusual, as $\rho$ is increasingly influenced by the presence of grain boundary (GB). The GB acts as a region of enhanced scattering for the conduction electron.[11] The estimated ratio of resistivity at the peak and that at lowest measuring temperature, viz. at 85 K

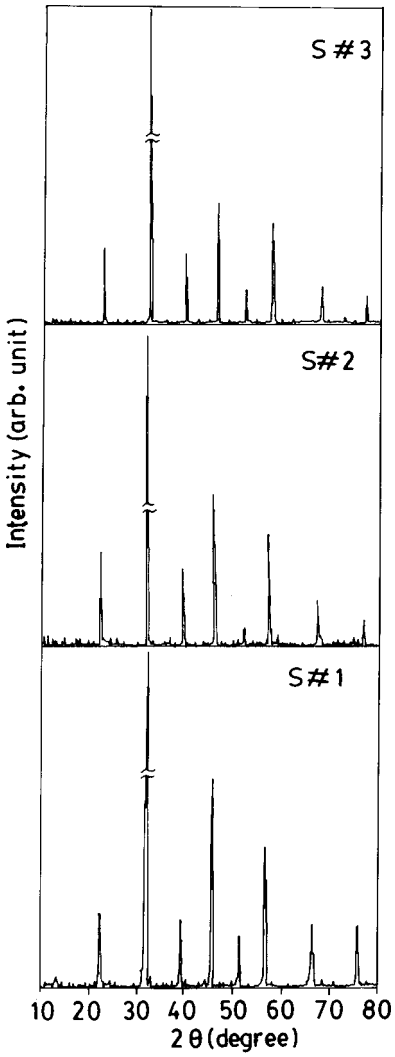


FIG. 1. XRD patterns of three $La_{0.5}Pb_{0.5}MnO_3$ samples with different grain sizes (S1 < S2 < S3) showing grain size dependent metal–insulator transitions.

($=\rho_p/\rho_{85}$) increases with increasing particle size (Table I), which also confirms similar results reported earlier on other GMR samples.[9,10] It is further noticed from Fig. 3 that for each of the samples, magnetic field has the effect of uniformly decreasing resistivity and shifting of $T_p$ to a higher temperature region.

The observed grain size and magnetic field dependent resistivity (and magnetization) data can be qualitatively explained with the help of magnetic domain scattering at the boundary regions.[9,11,17] From a microscopic point of view, the present system of our investigation contains metallic ferromagnetic domains connected by paramagnetic insulating regions. As the grain size decreases, the relative contribution of the insulating region increases, making $\rho$ large and lowering $T_p$.[10] For the samples with larger grain sizes, the contribution from the insulating region is small and as a result, $\rho$ is smaller.[10] TEM micrographs shown in Fig. 2 clearly indicate that for sample S3 with the largest grain size, the interconnectivity between the grains is better than those of S1 and S2 having smaller grain sizes. Thus the relative contribution

TABLE I. Some important physical parameters of the $La_{0.5}Pb_{0.5}MnO_3$ sample prepared by varying annealing and grinding time (annealing time increases in order of increasing sample number).

| Sample No. | Mean grain size ($\mu$m) XRD | Mean grain size ($\mu$m) TEM | $T_p$ (K) | $\theta_D$ (K) | $\rho_{300\,K}$ ($\Omega$ cm) | $\chi\times10^4$ (cgs) | $\rho_p/\rho_{85\,K}$ | $r_p$ (Å) |
|---|---|---|---|---|---|---|---|---|
| S1 | 0.019 | 0.102 | 235 | 598 | 1.158 | 46.825 | 1.48 | 1.89 |
| S2 | 0.036 | 0.139 | 259 | 608 | 0.401 | 48.899 | 1.85 | 2.08 |
| S3 | 0.039 | 0.229 | 280 | 640 | 0.215 | 61.701 | 2.27 | 2.09 |

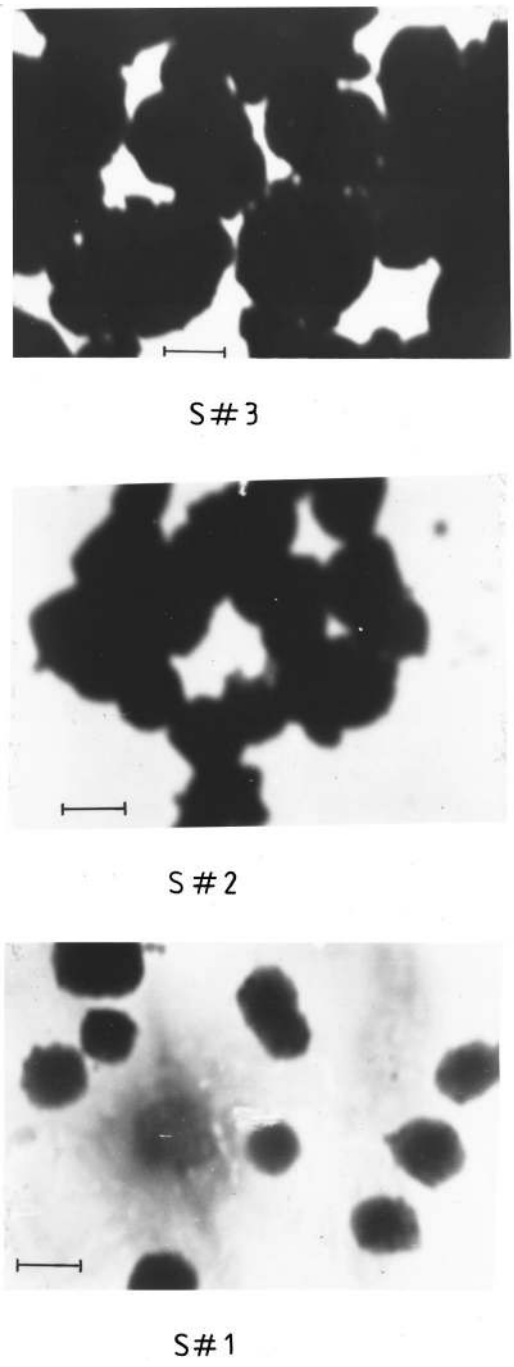


FIG. 2. TEM micrographs of three $La_{0.5}Pb_{0.5}MnO_3$ samples of different grain sizes (S1, S2, and S3). Bar indicates $10^{-5}$ cm.

of the insulating region connecting the grains is smaller in the sample with a bigger grain size, which is also in accordance with our explanation. Considering the electronic structure of $Mn^{3+}$ $[t_{2g}^3, e_g^1(S=2)]$ and $Mn^{4+}$ $[t_{2g}^3(S=3/2)]$, it is well known that the $e_g^1$ electron of $Mn^{3+}$ is only electronically active. Since the conduction electrons are completely polarized inside a magnetic domain, these $e_g^1$ electrons are easily transferred between pairs of $Mn^{3+}$ and $Mn^{4+}$. When these electrons travel across the grains, strong spin dependent scattering at the GB will lead to high zero field $\rho$. Application of a magnetic field can readily align the domain into parallel configuration causing $\rho$ to drop, as seen from Fig. 3.

The temperature dependence of MR ratio $[\Delta\rho/\rho_0 = -(\rho_H-\rho_0)/\rho_0$, where $\rho_0$ is the zero field resistivity and $\rho_H$ is the resistivity in the applied field of $B=1.5$ T] of the

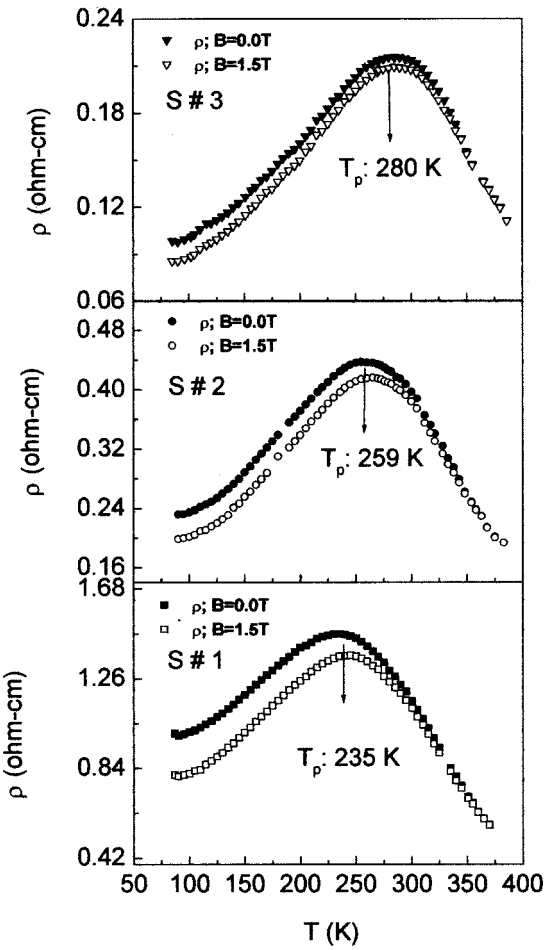


FIG. 3. Temperature dependent resistivity curves of three $La_{0.5}Pb_{0.5}MnO_3$ of different grain sizes S1, S2, and S3 (both in the presence and absence of magnetic field $B=0.0$ and $B=1.5$ T).

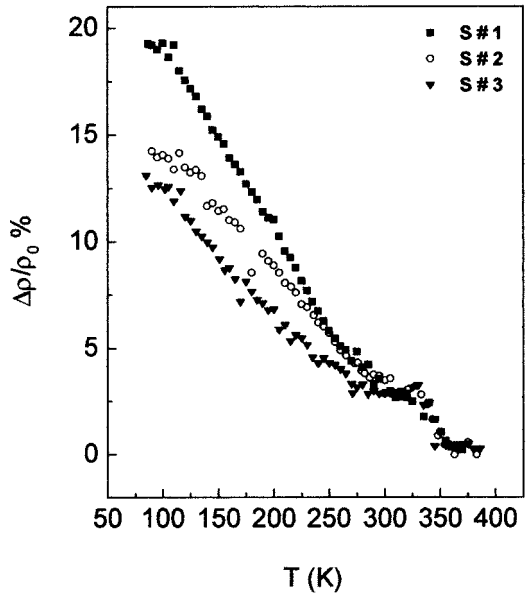


FIG. 4. Thermal variation of MR of the three $La_{0.5}Pb_{0.5}MnO_3$ samples of different grain sizes.

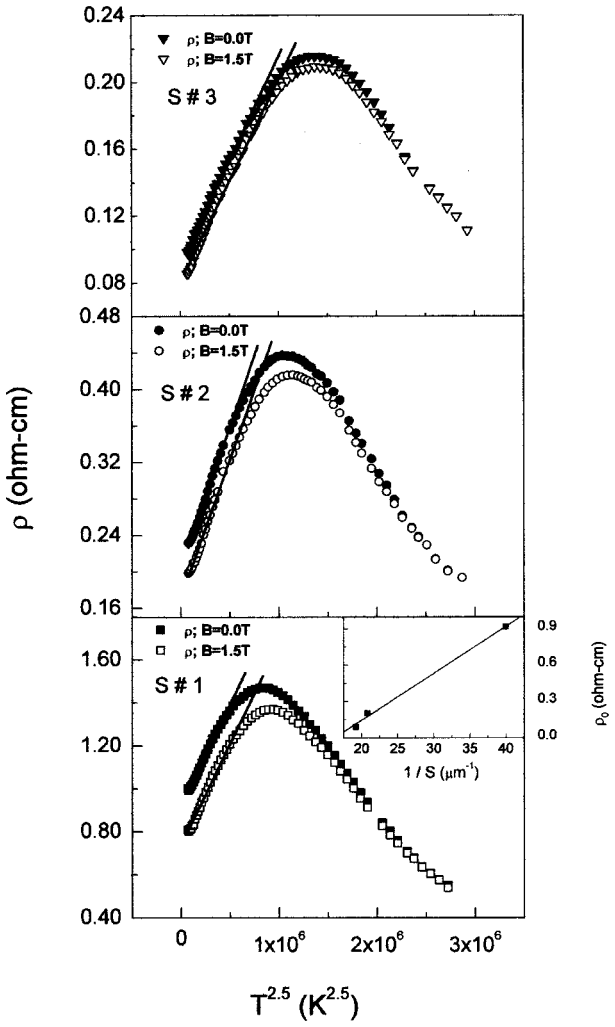


FIG. 5. Resistivity $\rho$ vs $T^{2.5}$ curves for three $La_{0.5}Pb_{0.5}MnO_3$ samples of different grain sizes (S1, S2, S3) both in the presence and absence of magnetic field. The solid lines indicate the best fit to the equation $\rho=\rho_0+\rho_{2.5}T^{2.5}$ at lower temperatures ($T<T_p$). Inset shows the variation of residual resistivity $\rho_0$ as a function of inverse grain size.

samples with different grain sizes are plotted in Fig. 4. The nature of thermal variations of the MR curves and the corresponding magnitudes of the MR values of the present samples are comparable to those obtained by other research groups[18] on similar samples. Although all the parameters, viz. $\rho$, $\rho_p/\rho_{85}$, $\chi$, and $T_p$ are markedly affected by the grain size, it is interesting to note that the peak value of MR as well as the corresponding peak temperature do not show significant change with grain size. The peak associate with the insulating paramagnetic to ferromagnetic metallic transition in the MR curve arises due to magnetic ordering between $Mn^{3+}$ and $Mn^{4+}$ (or the ratio of $Mn^{3+}/Mn^{4+}$ ions) and does not depend much on the grain size. This signifies that the ratio of $Mn^{3+}$ and $Mn^{4+}$ is comparable and almost equal to each other (i.e., it does not vary with grain size). Therefore the observed changes of transport properties of the same $La_{0.5}Pb_{0.5}MnO_3$ sample with different grain sizes could be attributed to the grain size effect, since the sample to sample variation of the ratio $Mn^{3+}/Mn^{4+}$ in general responsible for the changes of the said properties, was eliminated.[9,19] Figure 4 also indicates that the change of MR is larger for samples with smaller sizes and in the high temperature semiconducting region ($T>T_p$) this change is negligible. It is interesting to mention here that the low temperature ($T<T_p$) MR of a single crystal of GMR material is also found to be very small.[11] This implies that a substantial part of the MR of the present samples, at low temperature, arises from the grain boundaries which was also pointed out by Mahesh and a co-worker.[9]

From the analysis of the low temperature ($T<T_p$) resistivity data (ferromagnetic part), it appears that the grain size and domain scattering at the grain boundary regions are related. From the survey of recent literature,[20–25] it is found that the temperature dependent resistivity data in this region have not yet been well understood. The low temperature transport property is affected by several factors, viz. impurity, complicated band structure, electron–electron, electron–magnon scattering, etc. Snyders *et al.*[20] and Urushibara *et al.*[24] tried to explain the resistivity data in the low temperature regime with the help of an electron–electron ($\sim T^2$ dependency) scattering term. These authors[20] also included an additional $T^{4.5}$ contribution, which was considered to be an electron–magnon scattering term. But, on the other hand, Urushibara showed that this contribution is actually due to spin wave scattering and the electron–magnon scattering process shows a $T^{2.5}$ dependency. To justify the magnon scattering contribution, similar to earlier work[13,14] on the $La_{0.5}Pb_{0.5}Mn_{1-x}Cr_xO_3$ type samples, we have fitted the low temperature resistivity data ($T<T_p$) for the present set of $La_{0.5}Pb_{0.5}MnO_3$ samples with different equations having $T^2$, $T^{2.5}$, and $T^2+T^{4.5}$ dependencies of resistivity. It is observed that the equation $\rho=\rho_0+\rho_{2.5}T^{2.5}$ best fits the low temperature resistivity data of all the present samples. Figure 5 shows that the $\rho\sim T^{2.5}$ curves (for both $B=0.0$ and 1.5 T) are almost linear. This confirms that the transport mechanism in the low temperature ($T<T_p$) region is primarily due to the

TABLE II. The values of the parameters $\rho_0$, $\rho_{2.5}$, and activation energy $E_p$ [Eq. (1)] obtained from fitting the low temperature ($T<T_p$) and high temperature ($T>\theta_D/2$) conductivity data both in the presence and absence of magnetic field.

| Sample No. | $\rho_0$ ($\Omega$ cm) | | $\rho_{2.5}$ ($\Omega$ cm K$^{-2.5}$) | | $E_p$ (meV) | |
|---|---|---|---|---|---|---|
| | 0.0 T | 1.5 T | 0.0 T | 1.5 T | 0.0 T | 1.5 T |
| S1 | 0.918 | 0.738 | $9.48\times10^{-7}$ | $9.41\times10^{-7}$ | 124.43 | 120.94 |
| S2 | 0.203 | 0.171 | $3.11\times10^{-7}$ | $3.02\times10^{-7}$ | 119.07 | 117.99 |
| S3 | 0.0961 | 0.081 | $1.25\times10^{-7}$ | $1.21\times10^{-7}$ | 107.83 | 105.94 |

electron–magnon scattering term, which further demonstrates that the metallic regime is actually in the ferromagnetic (FM) phase.[21] The temperature independent $\rho_0$ term stands for the residual resistivity and arises due to domain, grain boundary, and other temperature independent scattering terms.[20,23] The parameters obtained from the best fitted low temperature resistivity data are shown in Table II, both for $B=0.0$ and 1.5 T. As expected, the temperature independent residual resistivity term $\rho_0$ for all the present polycrystalline samples is somewhat larger than that obtained for single crystals.[25] One finds from Table II that $\rho_0$ and $\rho_{2.5}$ decrease with increasing grain size, both for $B=0.0$ and 1.5 T. It indicates that with increasing grain size, the grain boundary region of individual grains decreases (Fig. 2) and hence the net grain boundary scattering term, influencing both the residual resistivity $\rho_0$ and the electron–magnon scattering term $\rho_{2.5}$, decreases. This is in accordance with our earlier finding that $\rho$ is increasingly affected by the presence of a GB, which acts as the region of the enhanced scattering center for the conduction electron. Again for each of the samples with fixed average grain size, it is seen from Table II that both $\rho_0$ and $\rho_{2.5}$ decrease with increasing magnetic field. This is likely, due to the fact that the main mechanism responsible for magnetoresistance is the influence of magnetic field on the magnetic domains and hence on the grain size.[13,25] The magnetic field suppresses the scattering from the domain boundary, as the field can align the domain into a parallel configuration, causing $\rho$ and hence $\rho_0$ and $\rho_{2.5}$ to decrease with the application of the field as discussed above. The plot of residual resistivity $\rho_0$ as a function of inverse grain size shows a nearly linear curve (inset, Fig. 5). From the slope of the curve, the specific grain boundary resistivity is estimated to be $\sim 3.9\times10^{-6}$ $\Omega$ cm$^2$, which is 1 order of magnitude higher than that of La–Ca–Mn–O thin film.[11] This is considered to be due to the larger (1 order of magnitude) grain size of the film samples[11] than those of the present ceramic samples.

The signature of grain size effect is also visualized from the high temperature (above MIT temperature) resistivity data. It is observed from the analysis that these data can be well fitted with a thermally activated small polaron hopping (SPH) model,[26] similar to other samples[3,20,21,27] of the GMR family. According to the SPH model,[26] the expression for resistivity is given by

$$\rho/T=\rho_\alpha \exp(E_p/k_BT), \tag{1}$$

where $\rho_\alpha=[k_B/\nu_{\rm ph}Ne^2R^2c(1-c)]\exp(2\alpha R)$; $k_B$ is the Boltzmann constant, $T$ is the absolute temperature, $N$ is the number of ion sites per unit volume (calculated from density data), $R$ is the average intersite spacing obtained from the relation $R=(1/N)^{1/3}$, $c$ is the fraction of sites occupied by a polaron, $\alpha$ is the electron wave function decay constant, and $\nu_{\rm ph}$ is the optical phonon frequency. $E_p$ is the activation energy given by the relation[28] $E_p=W_H+W_D/2$ for $T>\theta_D/2$ (and $E_p=W_D$ for $T<\theta_D/4$), where $W_H$ is the polaron hopping energy given by $E_p-E_s$ (discussed later), $W_D$ is the disorder energy, and $\theta_D$ is the Debye temperature. Resistivity curve (for both $B=0.0$ T and 1.5 T) are replotted as $\ln(\rho/T)$ versus $1/T$ in Fig. 6. The nature of these curves confirms the applicability of Mott's SPH model in the insulating (semiconducting) region (above $\theta_D/2$) predicting temperature dependence of activation energy in this region. From the slope of the straight line above $\theta_D/2$ [obtained by fitting the resistivity curve with Eq. (1)], we have estimated the activation energy. The values of $\theta_D/2$ are obtained as usual from the temperature, where deviation from linearity occurs in the high temperature region as shown in Fig. 6. The model parameters presented in Table II indicate that with increasing grain size, the activation energy gradually decreases both in the presence and absence of the magnetic field. This can be explained on the basis of the fact that with increasing grain size interconnectivity between grains increases (see TEM micrographs in Fig. 2), which help $e_g^1$, the only active electron, to hop between neighboring sites with much ease. This also explains the decrease of activation energy $E_p$ with the gradual increase of grain size. It is well known[26] that conductivity data of semiconducting oxide system in the low temperature regime (below $\theta_D/2$) follow Mott's variable range hopping (VRH) model of charge carriers. Recently, working with similar manganite systems, like La–Sr–Mn–Cu–O and La–Ca–Mn–O, different research groups[21,29,30] applied the VRH model to fit the conductivity data through the entire high temperature range ($T>T_p$). Here we should point out that the said VRH model [Eq. (2) shown below] was actually derived for explaining the conductivity data below $\theta_D/2$ (see straight line part in Fig. 7).[26] Accordingly, it is not generally appropriate to apply the VRH model for all the temperatures above $T_p$. For this reason, similar to our earlier work,[13] we applied the VRH model to fit the experimental data only in the lower temperature part of the high temperature conductivity data of the present samples, i.e., between

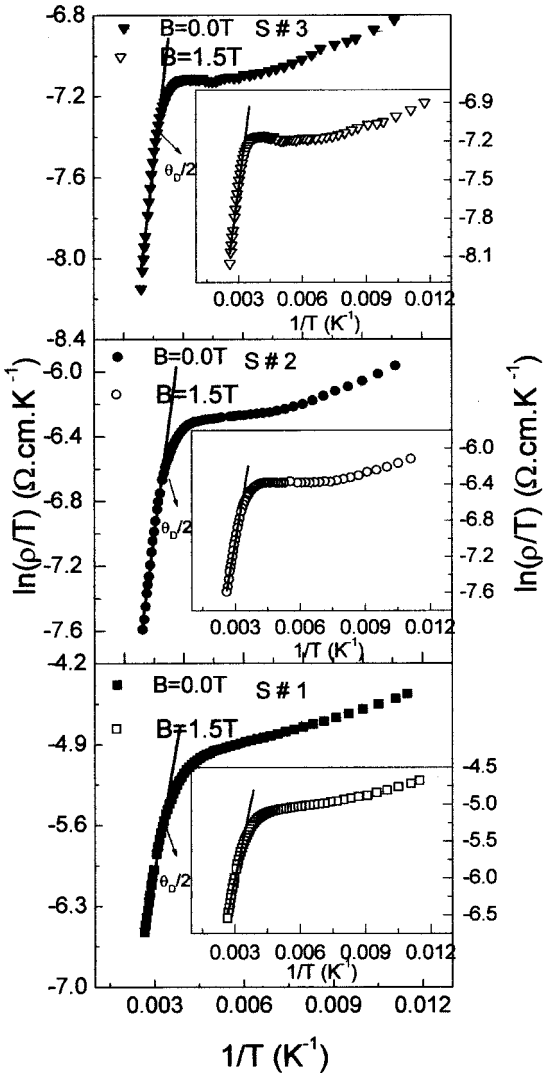


FIG. 6. Variation of $\ln(\rho/T)$ as a function of inverse temperature $(1/T)$ of $La_{0.5}Pb_{0.5}MnO_3$ with different grain sizes S1, S2, and S3. The insets represent the data taken in the presence of magnetic field $B=1.5$ T. Solid lines are the best fit to Mott's SPH model [Eq. (1)] above $\theta_D/2$.

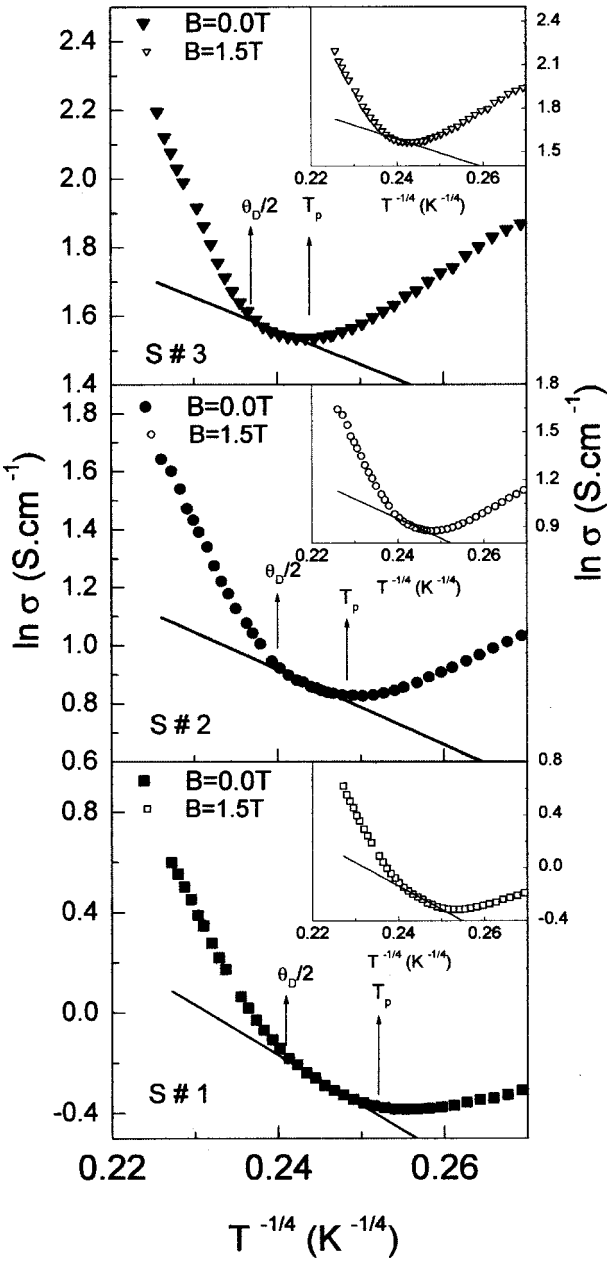


FIG. 7. Plot of $\ln\sigma$ vs $T^{1/4}$ for the sample $La_{0.5}Pb_{0.5}MnO_3$ with three different grain sizes (insets are the same curves with data taken in presence of magnetic field $B=1.5$ T). The solid lines indicate the best fits with Mott's VRH model [Eq. (2)]. The temperature range between $T_p$ and $\theta_D/2$ (where VRH is well satisfied) decreases with the increase of grain size in the sample.

$T_p$ and $\theta_D/2$, both for $B=0.0$ and 1.5 T. In the three dimensional case, the dc conductivity data according to the VRH model follows the equation[26]

$$\sigma=\sigma_0\exp(-[T_0/T])^{1/4}, \tag{2}$$

where $T_0$ is a constant$=16\alpha^3/k_BN(E_F)$, and $N(E_F)$ the density of states (DOS) at the Fermi level. $T_0$ is obtained from the slope of the $\ln\sigma$ versus $T^{-1/4}$ curve. The straight line of Fig. 7 gives the best-fit line obtained from fitting the conductivity data with Eq. (2). The values of $T_0$ given in Table III show that $T_0$ decreases with increasing grain size, both for $B=0.0$ and 1.5 T. But for a particular grain size, we notice that $T_0$ decreases with the application of magnetic field. It is related to suppression of the magnetic domain scattering with the application of the field, as discussed previously. From the value of $T_0$, we have also calculated DOS at the Fermi level, $N(E_F)$ (Table III) using the values of $\alpha=2.22\ \mathrm{nm}^{-1}$ (Ref. 13) and $2.25\ \mathrm{nm}^{-1}$ (Ref. 15) estimated earlier for similar GMR oxide samples. It is observed that $N(E_F)$ has an increasing trend with the increase of grain size (Table III). Careful examination of the best fit curve shown in Fig. 7 reveals that the temperature range over which VRH is applied (between $\theta_D/2$ and $T_p$), decreases (or the SPH conduction regime increases) with increase of grain size. Such a change in the nature of the hopping mechanism was also reported elsewhere.[21] Interesting information supporting the conduction mechanism, as discussed above, and the effect of grain size on transport properties are also obtained from the TEP data discussed below.

TABLE III. The values of different parameters obtained from fitting the VRH model [Eq. (2)] of the conductivity curve in the region $T_p < T < \theta_D/2$.

| Sample No. | $T_0$ | | $N(E_f)$ ($eV^{-1}\,cm^{-3}$) for $\alpha = 2.22\ nm^{-1}$ | | $N(E_f)$ ($eV^{-1}\,cm^{-3}$) for $\alpha = 2.25\ nm^{-1}$ | |
|---|---|---|---|---|---|---|
| | 0.0 T | 1.5 T | 0.0 T | 1.5 T | 0.0 T | 1.5 T |
| S1 | $15.9\times10^4$ | $9.8\times10^4$ | $1.24\times10^{22}$ | $2.01\times10^{22}$ | $1.82\times10^{22}$ | $2.95\times10^{22}$ |
| S2 | $2.8\times10^4$ | $2.4\times10^4$ | $7.08\times10^{22}$ | $8.39\times10^{22}$ | $1.08\times10^{23}$ | $1.23\times10^{23}$ |
| S3 | $0.9\times10^4$ | $0.8\times10^4$ | $2.12\times10^{23}$ | $2.32\times10^{23}$ | $3.11\times10^{23}$ | $3.40\times10^{23}$ |

### B. Grain size and field dependent thermoelectric power

It should be noted that strong temperature dependence of thermoelectric power (Seebeck coefficient $S$) for manganite samples with varying grain size has not been analyzed in detail to date.[10] Temperature dependence of $S$ (both at $B = 0.0$ and 1.5 T) for two typical samples S1 and S3 of different grain sizes (S3 > S1) is shown in Fig. 8. The magnitude of $S$ and nature of the curve obtained at zero field agree very well with other reported[31] results. From Fig. 8 we find that though small, $S$ depends on grain size both in magnitude and in its temperature dependent behavior. In the more metallic sample (S3 with larger grain size), having low resistivity, the TEP in the low temperature metallic part is comparatively smaller ($S < 2\ \mu V$) than that ($S > 2\ \mu V$) obtained for the high resistive and small grain size sample (S1). This observation also supports the result of Mahendiran and co-workers.[10] Furthermore, it is observed that magnetic field dependency of TEP data increases with increasing grain size, i.e., TEP data of S3 is more field dependent than those of S1 with smaller grain size (Fig. 8). It is also interesting to note that TEP for S3 changes sign around 200 K, whereas TEP data of S1 changes sign at much higher temperature (~250 K). Figure 8 shows that for both the samples S1 and S3, TEP increases with magnetic field at low temperature, which also support the results obtained with other magnetoresistive samples.[29,32] The field dependent TEP data of sample S1 with smaller grain size also show a change in its field dependency at ~200 K. It is discussed below that the field dependent TEP data in the low temperature ferromagnetic region also show the signature of magnon contribution.

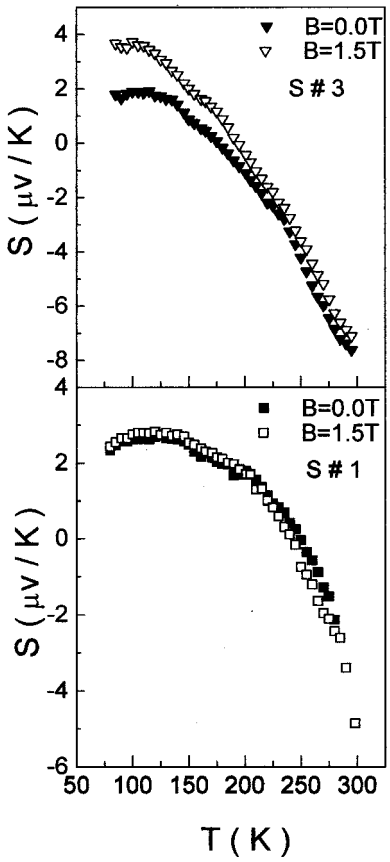


FIG. 8. Thermal variation of Seebeck coefficient $S$ of $La_{0.5}Pb_{0.5}MnO_3$ with two different grain sizes S1 and S3 (both at 0 and 1.5 T magnetic field). For the sample with smaller grain size (S1) the field dependence is very small particularly at the low temperature metallic regime.

Like low temperature ($T < T_p$) resistivity data, TEP data (for both $B = 0.0$ and 1.5 T) in the low temperature regime (ferromagnetic phase) were fitted with the following equation:[14,31]

$$S = S_0 + S_{1.5}T^{1.5} + S_4T^4, \tag{3}$$

where $S_0$ ($S$ at $T = 0$ K) has actually no physical origin. The $T^{1.5}$ behavior suggests that electron–magnon scattering dominate the low temperature TEP data (FM phase) in the present manganite system as in the case of resistivity[14,31] discussed earlier. The origin of the additional term $S_4T^4$ (not used to fit the corresponding resistivity data) required to fit the TEP data is considered to be due to spin wave fluctuation in the FM phase.[14] No such behavior is, however, detected from the resistivity data. Figure 9 shows the best fit curve [solid line obtained from fitting with Eq. (3)] in the low temperature metallic (ferromagnetic) phase of the $La_{0.5}Pb_{0.5}MnO_3$ samples. The corresponding fitting parameters, shown in Table IV indicate that $S_0$ and $S_{1.5}$ decrease with increasing grain size (for $B = 0.0$). This is likely to be due to the same magnetic domain and GB scattering mechanism discussed previously in analyzing resistivity data of the samples. The magnitude of the spin wave fluctuating parameter $S_4$ increases with the increase of grain size (at $B = 0.0$) as the large grain size contains a relatively larger number of fluctuating magnetic spins. It is found that compared to the model parameters fitting the resistivity data (Table II), the corresponding parameters fitting the TEP data (Tables IV and V) are less effected by different grain sizes and magnetic field strengths. It resembles the fact that thermopower is comparatively less sensitive to the grains, since heat flow from grain to grain is additive in nature.[14]

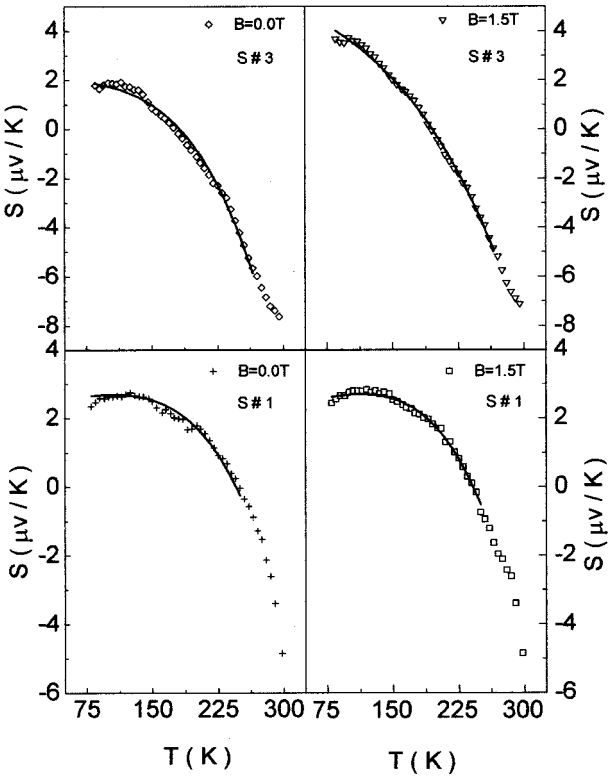


FIG. 9. Plot of $S$ as a function of temperature for $La_{0.5}Pb_{0.5}MnO_3$ with two different grain sizes S1 and S3 (both in the presence and absence of magnetic field). The solid lines represent the best fitting curves with the equation $S=S_0+S_{1.5}T^{1.5}+S_4T^4$.

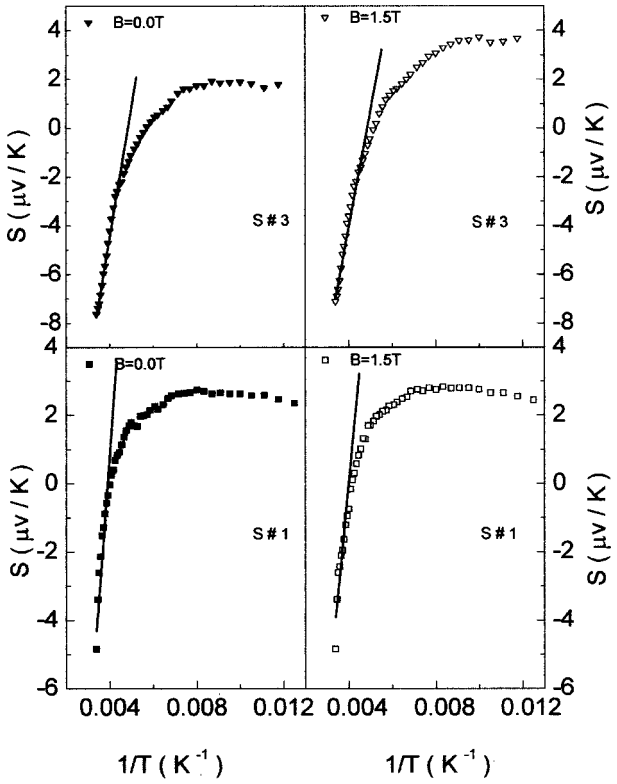


FIG. 10. Variation of thermopower $S$ as a function of inverse temperature $1/T$ for two $La_{0.5}Pb_{0.5}MnO_3$ with different grain sizes (S1 and S3) both for the $B=0.0$ and 1.5 T field. Solid lines are the best fits to Mott's SPH model [Eq. (4)] at high temperature ($T>\theta_D/2$).

Recently extensive efforts have been made to discuss the polaronic transport in the high temperature ($T>T_p$) paramagnetic phase of the GMR system.[29,33] We also notice that like resistivity the high temperature TEP data fit very well with Mott's equation[26] of the Seebeck coefficient which has the form

$$S=k_B/e[E_s/k_BT+\alpha'], \tag{4}$$

where $E_s$ is the activation energy obtained from the TEP data. $\alpha'$ is a constant, where $\alpha'<1$ suggests hopping due to small polaron and $\alpha'>2$ suggests the existence of a large polaron.[14,34] The solid line in the $S$ versus $1/T$ plot (Fig. 10) gives the best fit curve to Eq. (4). From the slope of the curve we obtain $E_s$, activation energy from the TEP data for two typical samples of different grain size (S1 and S3). The parameter $\alpha'$, obtained from fitting the curves (both for $B=0.0$ and 1.5 T) are also shown in Table V for comparison. The values of $E_s$ obtained from TEP measurement (both for $B=0.0$ and 1.5 T) are nearly 1 order of magnitude smaller than those ($E_p$, Table II) obtained from the resistivity data. The reason for such a difference, as originally pointed out by Mott and Davis,[26] and also recently supported by others,[32,35] is due to the thermally activated nature of hopping transport at high temperature. The estimated value of hopping energy $W_H(=E_p-E_s)$, both obtained in the absence and in the presence of the field is presented in Table V. It is observed that all the parameters $E_p$, $E_s$, and $W_H$ decrease with increasing grain size. Moreover, for a particular grain size, the parameters $E_p$, $E_s$, and $W_H$ decrease with the application of magnetic field and can be similarly explained as in the case of resistivity discussed above in Sec. III A. Decrease of polaron hopping energy $W_H$ with field implies that polaronic radius $r_p$ increases with field indicated from the relation[26]

$$W_H=e^2/4\varepsilon(1/r_p-1/R), \tag{5}$$

where the polaronic radius $r_p$ varies inversely with $W_H$. From the calculated values of $\alpha'$ (Table V), for $B=0.0$ and 1.5 T, it is seen that $\alpha'<1$. This supports the validity of small polaron hopping conduction[34] in the system of our

TABLE IV. The values of the parameters $S_0$, $S_{1.5}$, and $S_4$ obtained from fitting the low temperature (ferromagnetic phase) thermoelectric power data [Eq. (3)] both in the presence and absence of magnetic field.

| Sample No. | $S_0$ ($\mu$V/K) | | $S_{1.5}$ ($\mu$V/K$^{5/2}$) | | $S_4$ ($\mu$V/K$^5$) | |
|---|---|---|---|---|---|---|
| | 0.0 T | 1.5 T | 0.0 T | 1.5 T | 0.0 T | 1.5 T |
| S1 | 2.479 | 2.365 | $3.1\times10^{-4}$ | $4.4\times10^{-4}$ | $-1.01\times10^{-9}$ | $-1.18\times10^{-9}$ |
| S3 | 2.109 | 5.265 | $-2.2\times10^{-4}$ | $-15.5\times10^{-4}$ | $-1.43\times10^{-9}$ | $-0.71\times10^{-9}$ |

TABLE V. The values of activation energies and other related parameters estimated from high temperature thermoelectric power data [Eq. (4)] of different $La_{0.5}Pb_{0.5}MnO_3$ samples, both in the presence and absence of magnetic field. $E_p$ values of Table II are used.

| Sample No. | $E_s$ (meV) | | $W_H = E_p - E_s$ (meV) | | $\alpha'$ | |
|---|---|---|---|---|---|---|
| | 0.0 T | 1.5 T | 0.0 T | 1.5 T | 0.0 T | 1.5 T |
| S1 | 8.54 | 6.62 | 115.89 | 114.32 | −0.38 | −0.31 |
| S3 | 5.33 | 4.81 | 102.50 | 101.13 | −0.29 | −0.27 |

present investigation. Furthermore, the increase of $\alpha'$ with field also strongly supports our observation that $r_p$ increases with magnetic field, similar to the case of the Cr doped system studied earlier.[14] The estimated grain size dependent values of the polaronic radius[36] shown in Table I confirm that $r_p$ gradually increase with the increase of grain size.

We have attempted to whether determine the VRH mechanism is also supported from the TEP data. Similar to the resistivity data, the high temperature TEP data have been fitted with Mott's VRH equation for thermopower,[26] viz. $S = k_B{}^2/2e[(T_0T)^{1/2}(d \ln N/dE)]$. Figure 11 shows the $S-T^{1/2}$ curve for two typical $La_{0.5}Pb_{0.5}MnO_3$ samples of different grain sizes (S1 and S3). Interestingly, we notice no evidence of $T^{1/2}$ dependency of $S(T)$ data in the said temperature range where the VRH model the corresponding resistivity data. The origin of this discrepancy was also pointed out by other researchers.[32,35] However, the total scenario of the different behavior of TEP from that of resistivity is still not clear and needs further study.

## IV. SUMMARY AND CONCLUSION

The electrical conductivity data of the La–Pb–Mn–O type manganite system is highly sensitive to the grain size. Thermoelectric power is, however, comparatively less sensitive to the change of grain size since heat flow from grain to grain is additive in nature. Room temperature paramagnetic susceptibility of all the sample increases (while resistivity decreases) with the increase of grain size. In the insulating (semiconducting) regime ($T > T_p$), polaron hopping (for $T > \theta_D/2$) is valid for all the samples. With the increase of grain size, the temperature range of the validity of the VRH conduction mechanism decreases. The temperature width $\Delta T(=T_p - \theta_D/2)$ is larger for the sample with smaller grain size. In the presence of magnetic field $\Delta T$ remains almost unchanged. Since the thermopower is less effected by the grain size of the samples, the small polaron and variable range hopping regions are difficult to distinguish from the TEP data. This might be the reason why the VRH mechanism is not clear from the TEP data (both in the presence and absence of magnetic field) though this mechanism is satisfied by the resistivity data. From fitting of the conductivity data in the insulating (semiconducting for $T > T_p$) region, we come to the conclusion that both hopping energy $W_H$ decrease and polaron radius $r_p$ increase with the increase of grain size, even in the presence of magnetic field. Although the magnetic field dependent $S$ is small it is larger in samples with larger grain size. Both resistivity and TEP data in the low temperature ($T < T_p$) confirm the importance of magnon-carrier scattering. The parameters fitting resistivity and thermoelectric power are also found to depend both on the grain size and the applied magnetic field. In addition to the magnon-scattering term fitting the resistivity data, a spin-wave fluctuating term is required to fit the TEP data in the low temperature ferromagnetic phase (both at $B = 0.0$ and 1.5 T). Further study is necessary to shed more light on the field and grain size dependent thermopower and conductivity of the rare-earth manganites.

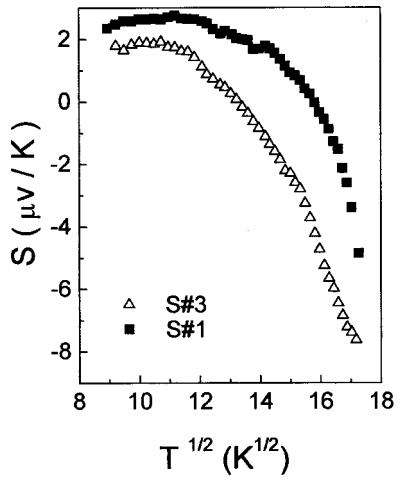


FIG. 11. Thermal variation of Seebeck coefficient $S$ as a function of $T^{1/2}$ of two $La_{0.5}Pb_{0.5}MnO_3$ samples with different grain sizes (S1 and S3) in the absence of magnetic field showing that in contrast to the resistivity data, validity of the VRH model cannot be justified from the TEP data.

## ACKNOWLEDGMENT

The authors are grateful to the Department of Science and Technology, Government of India for financial assistance.

[1] M. McCormack, S. Jin, T. H. Tiefel, R. M. Fleming, J. M. Phillips, and R. Ramesh, Appl. Phys. Lett. **64**, 3045 (1994).
[2] R. von Helmolt, J. Wecker, B. Holzapfel, M. Schultz, and K. Samwer, Phys. Rev. Lett. **71**, 2331 (1993).
[3] R. Mahendiran, R. Mahesh, A. K. RayChaudhuri, and C. N. R. Rao, J. Phys. D **28**, 1743 (1995).
[4] C. Zener, Phys. Rev. **82**, 403 (1951).
[5] A. J. Millis, P. B. Littlewood, and B. I. Shraiman, Phys. Rev. Lett. **74**, 5144 (1995).
[6] B. Chen, A. G. Rojo, C. Uher, H. L. Ju, and R. L. Greene, Phys. Rev. B **55**, 15471 (1997).
[7] M. Jaime, P. Lin, M. B. Salamon, and P. D. Han, Phys. Rev. B **58**, R5901 (1998).
[8] K. Chahara, T. Ohno, M. Kasai, and Y. Kozono, Appl. Phys. Lett. **63**, 1990 (1993).
[9] R. Mahesh, R. Mahendiran, A. K. RayChaudhuri, and C. N. R. Rao, Appl. Phys. Lett. **68**, 2291 (1996).

[10] R. Mahendiran, R. Mahesh, A. K. RayChaudhuri, and C. N. R. Rao, Solid State Commun. **99**, 149 (1996).
[11] A. Gupta *et al.*, Phys. Rev. B **54**, R15629 (1996).
[12] G. Ji, X. J. Fan, J. H. Zhang, C. S. Xiong, and X-G. Li, J. Phys. D **31**, 3036 (1998).
[13] A. Banerjee, S. Pal, and B. K. Chaudhuri, J. Chem. Phys. **115**, 1550 (2001).
[14] A. Banerjee, S. Pal, S. Bhattacharya, B. K. Chaudhuri, and H. D. Yang, Phys. Rev. B **64**, 104428 (2001).
[15] S. Pal, A. Banerjee, E. Rozenberg, and B. K. Chaudhuri, J. Appl. Phys. **89**, 4955 (2001).
[16] A. Taylor, *X-Ray Metallography* (Wiley, New York, 1961), p. 674.
[17] N. Zhang, W. Yang, W. Ding, D. Xing, and Y. Du, Solid State Commun. **109**, 537 (1999).
[18] X. Wen-xu, L. Bao-he, Q. Zheng-nan, and J. Han-min, J. Appl. Phys. **86**, 5164 (1999).
[19] G. H. Jonker and J. H. Van Santen, Physica (Amsterdam) **16**, 337 (1950).
[20] G. J. Snyder, R. Hiskes, S. DiCarolis, M. R. Beasley, and T. H. Geballe, Phys. Rev. B **53**, 14434 (1996).
[21] L. Pi, L. Zheng, and Y. Zhang, Phys. Rev. B **61**, 8917 (2000).
[22] H. Y. Hwang, S-W. Cheong, N. P. Ong, and B. Batlogg, Phys. Rev. Lett. **77**, 2041 (1996).
[23] J. M. De Teresa *et al.*, Phys. Rev. B **54**, 1187 (1996).
[24] A. Urushibara *et al.*, Phys. Rev. B **51**, 14103 (1995).
[25] P. Schiffer, A. P. Ramirez, W. Bao, and S.-W. Cheong, Phys. Rev. Lett. **75**, 3336 (1995).
[26] N. F. Mott and E. A. Davis, *Electronics Process in Non Crystalline Materials* (Clarendon, Oxford, 1971).
[27] R. Mahendiran, S. K. Tiwary, A. K. RayChaudhuri, T. V. Ramakrishnan, R. Mahesh, N. Rangavittal, and C. N. R. Rao, Phys. Rev. B **53**, 3348 (1996).
[28] G. N. Austin and N. F. Mott, Adv. Phys. **18**, 41 (1969).
[29] M. Jaime, M. B. Salamon, M. Rubinstein, R. E. Treece, J. S. Horwitz, and D. B. Chrisey, Phys. Rev. B **54**, 11914 (1996).
[30] M. Viret, L. Ranno, and J. M. D. Coey, Phys. Rev. B **55**, 8067 (1997).
[31] P. Mandal, Phys. Rev. B **61**, 14675 (2000).
[32] V. H. Crespi, L. Lu, Y. X. Jia, K. Khazeni, A. Zettl, and M. L. Cohen, Phys. Rev. B **53**, 14303 (1996).
[33] S. Chatterjee, P. H. Chou, C. F. Chang, I. P. Hong, and H. D. Yang, Phys. Rev. B **61**, 6106 (2000).
[34] K. Sega, Y. Kuroda, and H. Sakata, J. Mater. Sci. **33**, 1303 (1998).
[35] M. Jaime, M. B. Salamon, K. Pettit, M. Rubinstein, R. E. Treece, J. S. Horwitz, and D. B. Chrisey, Appl. Phys. Lett. **68**, 1576 (1996).
[36] V. N. Bogomolov, E. K. Kudinov, and Y. A. Firsov, Sov. Phys. Solid State **9**, 2502 (1968).